Review:

Application of Carbon Dots as Corrosion Inhibitor: A Systematic Literature Review

Muhamad Jalil Baari[1*] and Ravensky Yurianty Pratiwi[2]

[1]*Department of Chemistry, Faculty of Science and Technology, Universitas Sembilanbelas November Kolaka, Jl. Pemuda, Kolaka 93517, Indonesia*

[2]*Department of Chemistry Education, Universitas Islam Negeri Raden Fatah Palembang, Jl. Prof. KH Zainal Abidin Fikri Km 3.5, Palembang 30126, South Sumatera, Indonesia*

* ***Corresponding author:***

email: jalilbaari@gmail.com

Received: January 18, 2022
Accepted: May 9, 2022

DOI: 10.22146/ijc.72327

Abstract: *Corrosion is spontaneity and unavoidable reactions which cause degradation in the quality of the materials. Most industries have been harmed by the corrosion of manufacturing equipment. Several methods can be applied to control this problem. The use of corrosion inhibitors is an effective and practical way to decrease metal deterioration significantly. Many commercial inorganic and organic compounds are effective inhibitors, but most of them are not completely safe and relatively expensive. Carbon dots and their derivatives are potential compounds for resolving corrosion reactions on metal surfaces. Carbon dots can be synthesized from various natural sources to be more environmentally friendly. This systematic review aims to summarize the concept of corrosion, types of carbon dots-based corrosion inhibitor and their effectiveness on various metals, inhibition mechanism, surface analysis of the protected metals, kinetics, thermodynamics, and quantum computational chemistry studies. This review also presents the significance and the prospects of carbon dots-based corrosion inhibitors.*

Keywords: *corrosion; corrosion inhibitor; carbon dots; carbon steel; copper; aluminium*

■ INTRODUCTION

Metal/alloy is generally used as the primary material for manufacturing equipment in various industries. The most commonly used metals/alloys are steel, aluminium, and copper. Carbon steel is affordable alloy material with high-strength properties and ease of fabrication. It has been widely used as the main component of transportation pipelines, oil storage tanks, and other manufacturing equipment in the oil and gas industries [1-2]. Unfortunately, this material is very vulnerable corroded when exposed to a corrosive environment which affects the continuity of the industrial production system [3-4]. Corrosion is the crushing of material due to contact with an aggressive environment. The corrosion process on carbon steel forms an iron oxide in the surface sites that are not strongly attached. Then, it flakes off easily to solution-phase conducting metal depletion [5]. The degradation of metallic components in industries will disrupt manufacturing processes, storage, and shipment.

Aluminium and its alloys are known to be useful in many applications, such as electronic devices, household industries, aeronautical manufacture, and the food industry, due to their high electrical capacity, mechanical strength, malleability, relatively low price, and high energy density [6-8]. Although aluminium can form a stable and protective thin oxide film in the outer part, aluminium still undergoes corrosion after interacting with aggressive media [9]. Meanwhile, copper and its alloys have good mechanical properties and remarkable electrical and thermal conductivity. It has been widely applied in many industrial fields, including freshwater supply lines in the marine environment, heating equipment, and electronic field [10-11]. However, copper is relatively susceptible to

being corroded in seawater which contains various types of ions at high concentrations [12].

Controlling methods toward corrosion consist of selecting proper alloy, altering of corrosive environment, metallic and non-metallic coatings, painting, amalgamating the surface, anodic and cathodic protection, and introducing surface compressive stress [13]. Another way to mitigate metal deterioration by dint of corrosion is the addition of corrosion inhibitors. A corrosion inhibitor is a chemical compound that can retard the corrosion rate in the attacked material through adsorption on the material surface [14]. This compound establishes a thin protective layer on the surface [15]. It was usually added in small concentrations into the corrosive solution. The use of inhibitors is an effective and practical method for metal protection against corrosion in acid and saline solutions [16-18]. Protection of several types of metal like carbon steel [18-19], mild steel [20-21], copper [11,22], and aluminium [7,23] by corrosion inhibitors have been reported. However, synthetic organic and inorganic corrosion inhibitors generally still have toxicity to the environment. Besides that, they are carcinogenic for humans, thus endangering the survival of the living organisms and restricting their utilization [21]. Because of the weakness of these commercial corrosion inhibitors, many kinds of research tried to develop eco-friendly corrosion inhibitors from organic or natural sources.

Carbon is an abundant element in nature. It is considered to have weak fluorescence and low water solubility. There are several carbon allotropes, for instance, graphite, diamond, amorphous, glassy carbon, fullerene, lonsdaleite, aggregated diamond nanorod, and carbon nanofoam. However, recent studies have focused on applying carbon dots as one of the carbon-based fluorescent (FL) nanomaterials due to unique properties such as good solubility in water, low cytotoxicity, and strong/unique luminescence [24-25]. Another property of carbon dots (CDs) is good biocompatibility [14,26]. Those specific properties are often exploited to use CDs in bioimaging, biosensing, photocatalysis, biomedicine, optoelectronic devices, drug carriers, electroanalysis, and other biological fields [24,27-31]. Four classes of carbon nanomaterials or carbon dots are graphene quantum dots (GQDs), carbon nanodots (CNDs), polymer carbon dots (CPDs), and carbon quantum dots (CQDs) with sizes below 10 nm [32-33]. These materials can be synthesized through simple methods from various natural sources with long carbon chains, thus making living organisms safe. The precursors are commonly abundant in natural sources, relatively cheap, and renewable [34]. Meanwhile, doping processes by putting in heteroatoms effectively improve the unique properties of CDs like emission spectrum range, fluorescence phenomenon, corrosion inhibitor, and other features [35-36].

Several researchers have informed that solutions containing CDs can effectively reduce the corrosion rate on the metal surface. This is attributed to the hydrophilic functional groups from the CDs for attracting water molecules and trapping oxygen from the metal surface. Then, adsorbed oxygen molecules on the CDs surface are directly converted to water molecules utilizing the four-electron pathways for retarding the corrosion process [37]. Hence, this article review will describe metal corrosion, corrosion mechanism on metal, characterization of CDs, application of green modified nanoparticle carbons (carbon dots) as corrosion inhibitors on several types of metal, aggressive solutions, and optimum conditions that produce the highest efficiency. Inhibition mechanism, kinetics, thermodynamics, quantum computational chemistry studies, significance, and the prospects of carbon dots-based corrosion inhibitor were also mentioned.

■ METAL CORROSION AND ITS MECHANISM

Corrosion is a spontaneous chemical reaction to the metal. Metal corrosion is caused by electrochemical reactions in which oxidation and reduction occur at once on the different sites of a metal. Fast or slow reactions depend on the nature/composition of the metal and the environmental aggressiveness level [38]. In the oil and gas industry, the availability of metal/alloy is a primary requirement for pipeline construction. It is used to transport crude oil and wet gas from the oil wells to provide some advantages [39].

Meanwhile, crude oil and wet gas are non-corrosive substances for metal. But, during the transportation process, the pipeline is also passed by impurities, for instance, salts, dissolved gas, and microorganisms [17,40-41]. These impurities are the main cause of internal corrosion/deterioration when in contact with metal that is very vulnerable to being oxidized [42]. Consequently, this condition inflicts economic loss due to the high cost of repairs and cessation of operational activities. Besides that, the oil spill can pollute the environment. Hence, additional treatments are required to overcome those problems.

Metal immersed in the aggressive solution will trigger a severe oxidation reaction. The oxidation products are metal ions that move to an anode site on the metal surface. Some metal ions leave the surface to the solution phase, thus decreasing the thickness of the pipeline. Another process is the formation of metal oxides, metal sulfides, or metal carbonates on the surface, which produces brittle rust. At the same time, electrons move to the cathode site as an assembly point. Reduction reactions occur in this site after species in the solution phase accept electrons [43]. The oxidation process of several metals and the type of electron acceptor on the cathode are displayed in Fig. 1.

■ METHODOLOGY

The preparation method of this systematic review was based on preferred reporting items for systematic review and meta-analyses (PRISMA). Literature resources extensively were obtained from online databases and libraries, such as Google Scholar, Scopus, ScienceDirect, ResearchGate, SpringerLink, Wiley Online Library, PubMed, and ACS Publications. Searches used keywords like corrosion, corrosion inhibitors, carbon dots, inhibition mechanism, adsorption isotherm, kinetics study of adsorption, thermodynamics study of adsorption, and computational study of CDs-based corrosion inhibitors. The scheme of the review process is displayed in Fig. 2. Literature obtained was screened based on the publication period of 2017–2022, the specific utilization of carbon dots as corrosion inhibitors with proper and precise methods in corrosion inhibition analysis, and the natural sources or precursors for synthesizing carbon dots.

■ CHARACTERIZATIONS OF CARBON DOTS AND CORROSION INHIBITION TEST METHODS

The precursor structures and synthesis methods of the carbon dots-based corrosion inhibitors are summarized in Fig. 3. All synthesized CDs must be characterized to confirm their structures and properties.

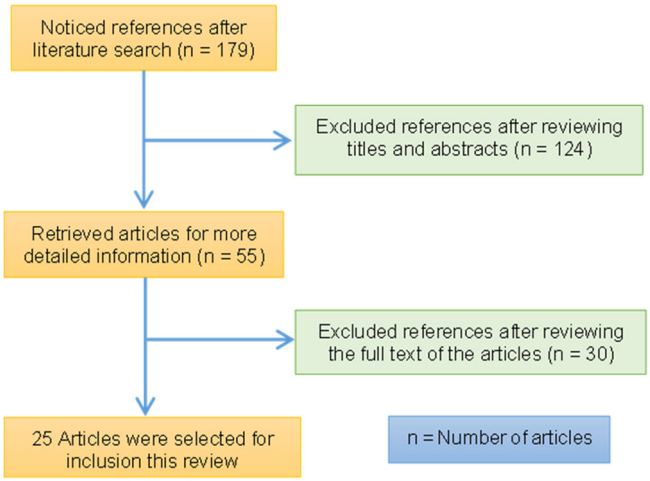

Fig 2. Scheme of the review process

Anode:

$Fe_{(s)} \rightarrow Fe^{2+}_{(aq)} + 2e^-$ (1)

$Al_{(s)} \rightarrow Al^{3+}_{(aq)} + 3e^-$ (2)

$Cu_{(s)} \rightarrow Cu^{2+}_{(aq)} + 2e^-$ (3)

Cathode:

$2H^+_{(aq)} + 2e^- \rightarrow H_{2(g)}$ (Acidic condition without oxygen) (4)

$O_{2(g)} + 2H_2O_{(l)} + 4e^- \rightarrow 4OH^-_{(aq)}$ (Neutral or basic condition by the presence of oxygen) (5)

$O_{2(g)} + 4H^+_{(aq)} + 4e^- \rightarrow 2H_2O_{(l)}$ (Acidic condition by the presence of oxygen) (6)

In saturated CO_2 solution, besides reaction Eq. (4), there are two reactions in cathode.

$2H_2CO_{3(aq)} + 2e^- \rightarrow H_{2(g)} + 2HCO_3^-$ (7)

$2HCO_3^-{}_{(aq)} + 2e^- \rightarrow H_{2(g)} + 2CO_3^{2-}{}_{(aq)}$ (8)

*Electrons that are produced in anode site will move to cathode site

Fig 1. The oxidation and reduction reactions of the corrosion process on the metal-solution interfaces

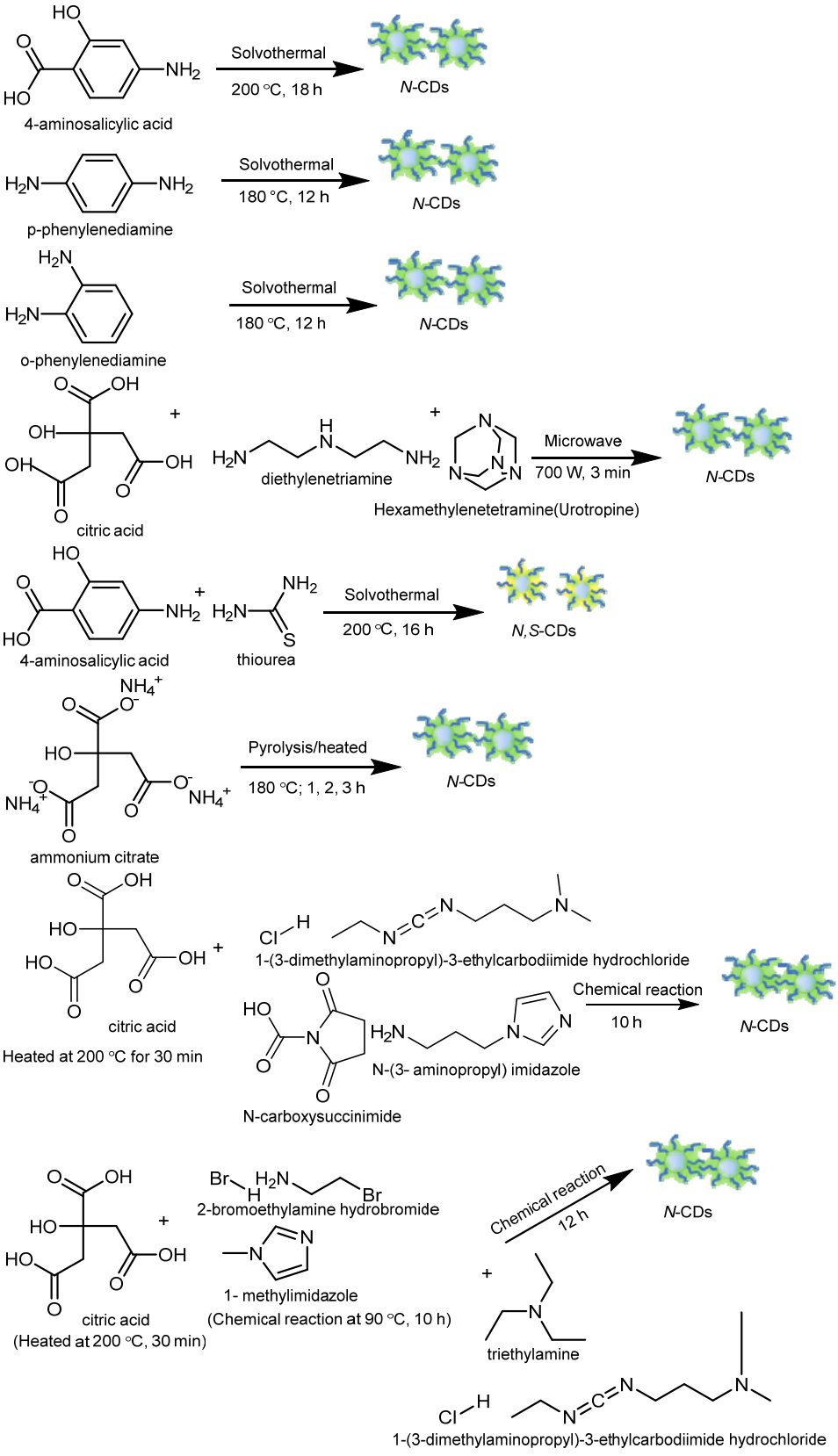

Fig 3. Precursor structures and synthesis schemes of carbon dots

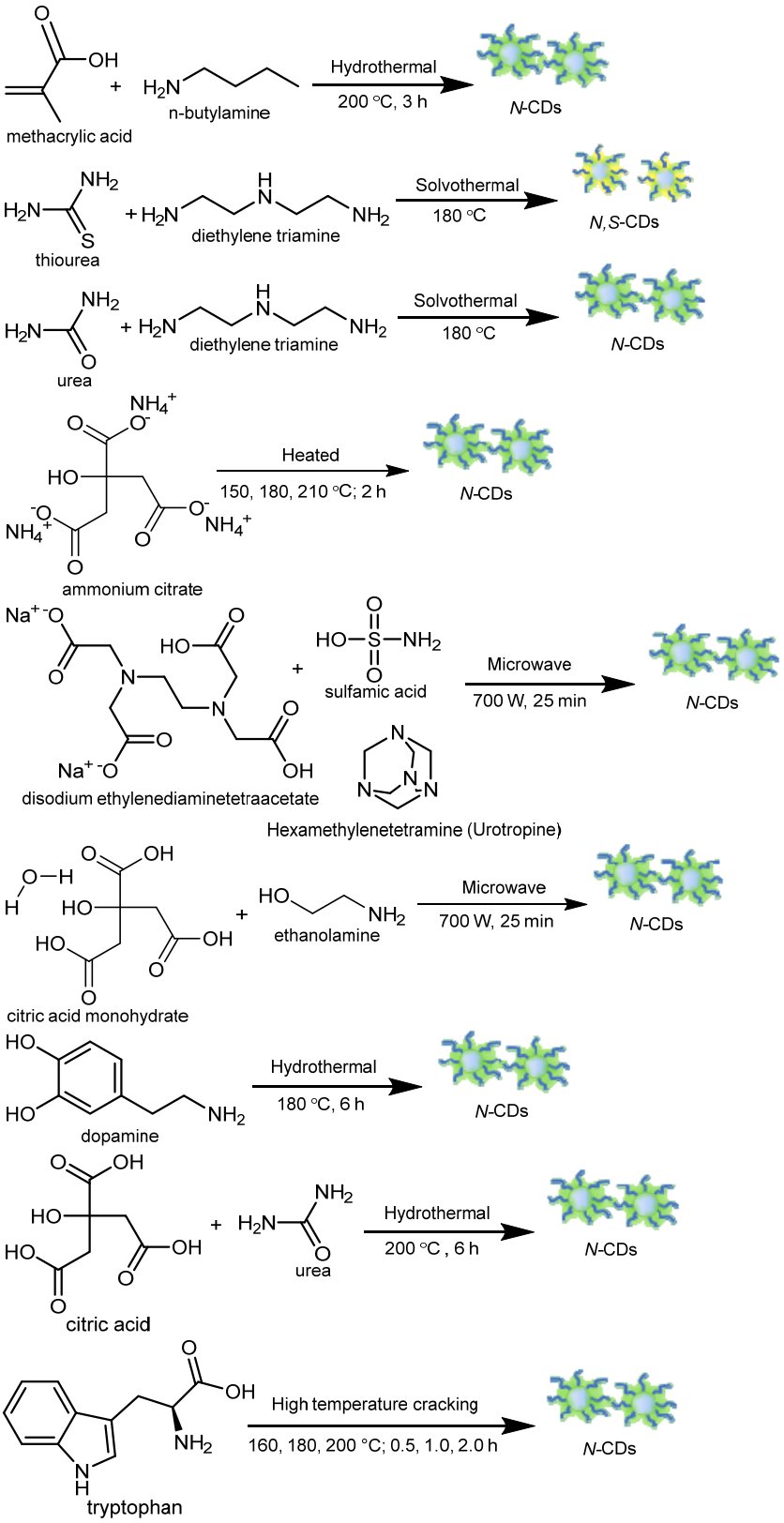

Fig 3. Precursor structures and synthesis schemes of carbon dots (*Continued*)

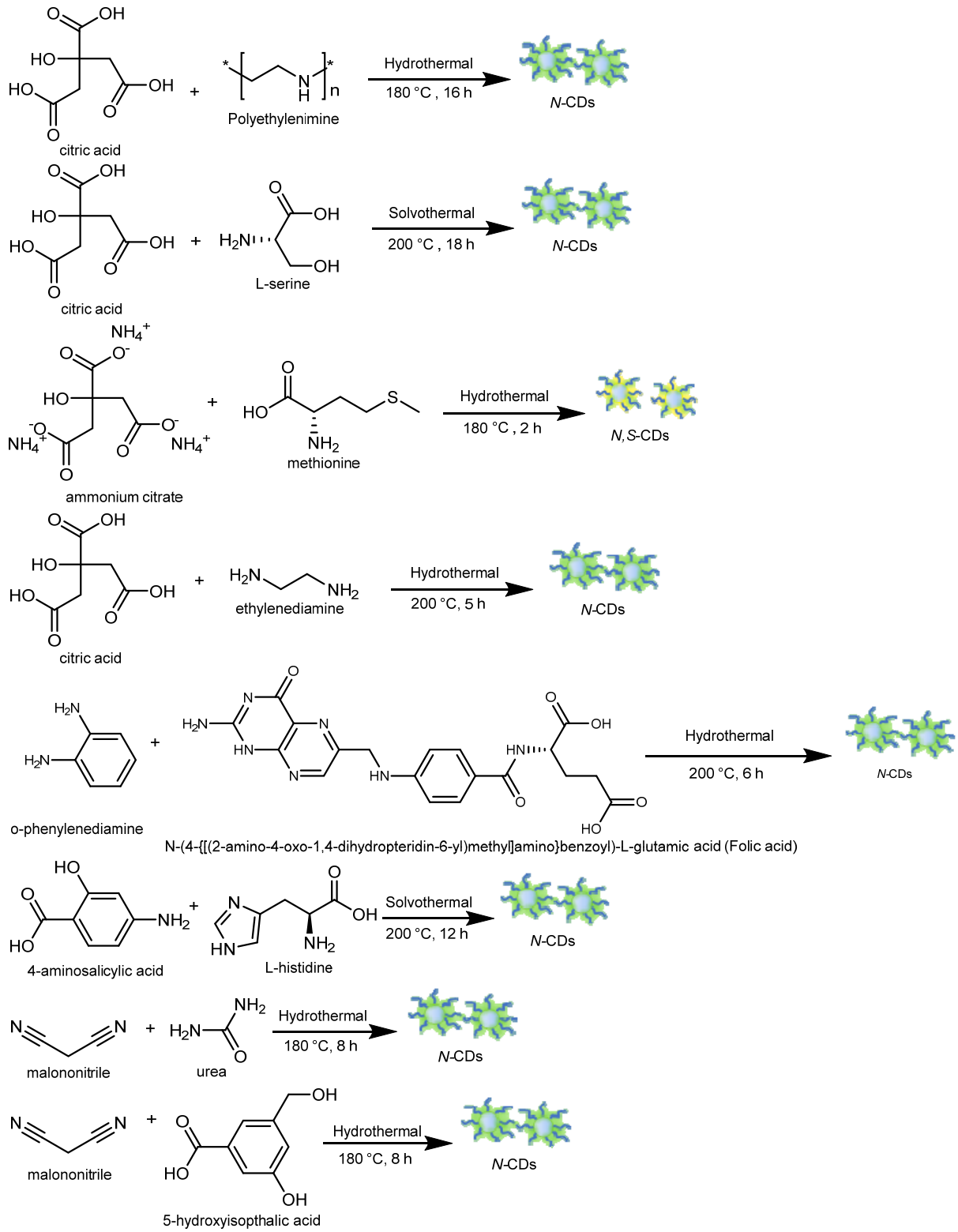

Fig 3. Precursor structures and synthesis schemes of carbon dots (*Continued*)

There are several methods that are commonly used. Characterizations of the chemical structures and luminescence properties are conducted by Fourier transform infrared (FTIR) and ultra violet-fluorescence

Table 1. Summary of details and research gaps for carbon dots-based corrosion inhibitors

No		Details	Gap	Ref.
1	a)	*N*-doped carbon dots from aminosalicylic acid (ASA)	Limitations: Constant temperature	[40]
	b)	Media: HCl 1 M solution		
	c)	Metal/alloy: Carbon steel	Remarks: Vary temperature	
	d)	Methods: Potentiodynamic polarization, EIS, weight loss, surface analysis (SEM and EDS)		
	e)	Parameters:		
		❖ Concentrations: 1, 5, 10, 50, 100 mg.L^{-1}		
		❖ Temperature: room temperature		
		❖ Immersion times: 0.5, 5, 10, 36, 52, 76, 88 h		
	f)	Results: Max IE: 96.00% (100 mg.L^{-1}, room temperature, 88 h, weight loss)		
2	a)	Carbon dots from durian juice	Limitations: Constant temperature and immersion time	[53]
	b)	Media: NaCl 1% solution		
	c)	Metal/alloy: Copper		
	d)	Methods: Potentiodynamic polarization and weight loss	Remarks: Vary temperature and immersion time	
	e)	Parameters:		
		❖ Concentrations: 200, 400, 500, 600, 700, 800 ppm		
		❖ Temperature: room temperature		
		❖ Immersion time: 14 days (weight loss)		
	f)	Results : Max IE: 86.00% (800 ppm, room temperature, potentiodynamic polarization)		
3	a)	*N*-doped carbon dots from p-phenylenediamine (p-PD) and o-phenylenediamine (o-PD)	Limitations: Constant temperature	[47]
	b)	Media: HCl 1 M solution	Remarks: Vary temperature.	
	c)	Metal/alloy: Carbon steel		
	d)	Methods: Potentiodynamic polarization, EIS, weight loss, surface analysis (SEM, LSCM, EDS)		
	e)	Parameters:		
		❖ Concentrations: 10, 50, 100, 200 mg.L^{-1}		
		❖ Temperature: room temperature		
		❖ Immersion times: 12, 24, 36, 48, 60, 72 h		
	f)	Results: Max IE : 97.00% for p-CDs, 99% for o-CDs (200 mg.L^{-1}, 72 h, 25 °C, weight loss)		
4	a)	*N*-doped carbon dots from citric acid, diethylenetriamine, and urotropine	Limitations: No information about temperature and immersion time variations in corrosion inhibition experiments	[14]
	b)	Media: HCl 1 M solution		
	c)	Metal/alloy: Carbon steel		
	d)	Methods: Potentiodynamic polarization, EIS, and weight loss		
	e)	Parameters:		
		❖ Concentrations: 50, 100, 200, 400, 600 ppm	Remarks: Vary immersion time and temperature on weight loss and electrochemical methods	
		❖ Temperatures: room temperature, 60 °C		
		❖ Immersion time: 0.5 h (open circuit potential)		
	f)	Results: Max IE: 84.93% (600 ppm, room temperature, EIS)		
5	a)	*N,S*-co-doped carbon dots from 4-aminosalicylic acid and thiourea	Limitations: Constant temperature	[23]
	b)	Media: HCl 0.1 M solution		
	c)	Metal/alloy: Aluminium	Remarks: Vary temperature	
	d)	Methods: Potentiodynamic polarization, EIS, weight loss, surface analysis (SEM, AFM, FTIR, IFM, XPS)		
	e)	Parameters:		

No	Details	Gap	Ref.
	❖ Concentrations: 1, 2, 3, 4, 5 mg.L^{-1} ❖ Temperature: 50 °C ❖ Immersion times: 1, 3, 6, 9, 12 h f) Results: Max IE: 95.22% (5 mg.L^{-1}, 50 °C, 3 h, EIS)		
6	a) *N,S*-co-doped carbon dots from 4-aminosalicylic acid and thiourea b) Media: CO_2-saturated NaCl 3.5% solution c) Metal/alloy: Carbon steel d) Methods: Potentiodynamic polarization, EIS, weight loss, surface analysis (SEM, AFM, XPS, and contact angle measurement) e) Parameters: ❖ Concentrations: 10, 20, 30, 40, 50 mg.L^{-1} ❖ Temperature: 50 °C ❖ Immersion times: 1, 3, 6, 9, 12 h f) Results: Max IE: 98.66% (50 mg.L^{-1}, 50 °C, 12 h, EIS)	Limitations: Constant temperature Remarks: Vary temperature	[4]
7	a) Functionalized carbon dots from citric acid, 1-(3-dimethylaminopropyl)-3-ethylcarbodiimide hydrochloride, N-carboxysuccinimide, N-(3-aminopropyl) imidazole, triethylamine b) Media: HCl 1 M solution c) Metal/alloy: Carbon steel d) Methods: Potentiodynamic polarization, EIS, weight loss, surface analysis (SEM) e) Parameters: ❖ Concentrations: 25, 50, 100, 200 mg.L^{-1} ❖ Temperature: 25 °C ❖ Immersion time: 24 h f) Results: Max IE: 94.00% (200 mg.L^{-1}, 25 °C, 24 h, potentiodynamic polarization)	Limitations: Constant temperature and immersion time Remarks: Vary temperature and immersion time	[54]
8	a) Functionalized carbon dots from citric acid, 2-bromoethylamine hydrobromide, 1- methylimidazole, 1-(3-dimethylaminopropyl)-3-ethylcarbodiimide hydrochloride, triethylamine b) Media: HCl 1 M solution and NaCl 3.5 % solution c) Metal/alloy: Q235 carbon steel d) Methods: Potentiodynamic polarization, EIS, weight loss, surface analysis (SEM, LSCM, EDS) e) Parameters: ❖ Concentrations: 25, 50, 100, 200 mg.L^{-1} ❖ Temperature: 25 °C ❖ Immersion times: 2, 6, 12, 24 h f) Results: ❖ Max IE in HCl 1 M: 92.60% (200 mg.L^{-1}, 25 °C, 24 h, Potentiodynamic polarization) ❖ Max IE in NaCl 3.5 % : 85.70% (200 mg.L^{-1}, 25 °C, 24 h, EIS)	Limitations: Constant temperature Remarks: Vary temperature	[50]
9	a) *N*-doped carbon dots from 4-aminosalicylic acid b) Media: H_2SO_4 0.5 M solution c) Metal/alloy: Copper d) Methods: Potentiodynamic polarization, EIS, weight loss, surface analysis (SEM, AFM, EDS) e) Parameters: ❖ Concentrations: 2, 5, 20, 50 mg.L^{-1} ❖ Temperatures: 25, 35, 45 °C	Limitations: Constant immersion time Remarks: Vary immersion time	[22]

No		Details	Gap	Ref.
		❖ Immersion time: 24 h		
	f)	Results:		
		Max IE = 91.10% (50 ppm, 25 °C, EIS)		
10	a)	*N*-doped carbon dots from ammonium citrate	Limitations: Constant temperature	[49]
	b)	Media: HCl 1 M solution		
	c)	Metal/alloy: Carbon steel	Remarks: Vary temperature	
	d)	Methods: Potentiodynamic polarization, EIS, weight loss, surface analysis (SEM, LSCM, XPS)		
	e)	Parameters:		
		❖ Concentrations: 50, 100, 150, 200 $mg.L^{-1}$		
		❖ Temperatures: 25 °C		
		❖ Immersion times: 2, 6, 12, 24, 48 h		
	f)	Results:		
		❖ Max IE: 96.96% (200 $mg.L^{-1}$, 25 °C, EIS)		
11	a)	*N*-doped carbon dots from methacrylic acid and n-butylamine	Limitations: Constant temperature	[44]
	b)	Media: HCl 1 M solution		
	c)	Metal/alloy: Carbon steel	Remarks: Vary temperature	
	d)	Methods: Potentiodynamic polarization, EIS, weight loss, surface analysis (SEM, LSCM, XPS, EDS, Raman spectroscopy)		
	e)	Parameters:		
		❖ Concentrations: 25, 50, 100, 200 $mg.L^{-1}$		
		❖ Temperature: 25 ± 5 ℃		
		❖ Immersion times: 6, 12, 24, 72, 120 h		
	f)	Results:		
		❖ Max IE: 99.35% (200 $mg.L^{-1}$, 25 ± 5 °C, 24 h, EIS)		
12	a)	*N,S*-co-doped carbon dots from thiourea and diethylene triamine	Limitations: No information about immersion time variations in corrosion inhibition experiments	[48]
	b)	Media: HCl 15 % solution		
	c)	Metal/alloy: Mild steel		
	d)	Methods: Potentiodynamic polarization, EIS, weight loss, surface analysis (SEM, AFM, XPS)	Remarks: Vary immersion time	
	e)	Parameters:		
		❖ Concentrations: 10, 25, 50, 75, 100 ppm		
		❖ Temperatures: 30, 40, 50, 60 °C		
		❖ Immersion time: -		
	f)	Results:		
		Max IE: 96.40% (100 ppm, 30 °C, weight loss)		
13	a)	*N*-doped carbon dots from urea and diethylene triamine	Limitations: No information about immersion time variations in corrosion inhibition experiments	[48]
	b)	Media: HCl 15 % solution		
	c)	Metal/alloy: Mild steel		
	d)	Methods: Potentiodynamic polarization, EIS, weight loss, surface analysis (SEM, AFM, XPS)	Remarks: Vary immersion time	
	e)	Parameters:		
		❖ Concentrations: 10, 25, 50,75, 100 ppm		
		❖ Temperatures: 30, 40, 50, 60 °C		
		❖ Immersion time: -		
	f)	Results:		
		Max IE: 90.80% (100 ppm, 30 °C, EIS)		
14	a)	*N*-doped carbon dots from ammonium citrate	Limitations: No information about temperature in experiments of corrosion inhibition	[45]
	b)	Media: HCl 1.0 M solution		
	c)	Metal/alloy: Q235 carbon steel		
	d)	Methods: Potentiodynamic polarization, EIS, weight loss, surface analysis (SEM, LSCM, XPS, Raman spectroscopy)	Remarks: Vary temperature	

No	Details	Gap	Ref.
	e) Parameters: ❖ Concentrations: 50, 100, 150, 200 ppm ❖ Temperature: - ❖ Immersion times: 2, 6, 12, 16, 24, 48 h f) Results: Max IE: 97.43% (200 ppm, potentiodynamic polarization, 24 h)		
15	a) *N*-doped carbon quantum dots from disodium ethylenediaminetetraacetate (EDTA), sulfamic acid, and urotropine b) Media: Saturated CO_2 3% NaCl solution c) Metal/alloy: N80 carbon steel d) Methods: Potentiodynamic polarization, EIS, weight loss, surface analysis (SEM, EDS) e) Parameters: ❖ Concentrations: 50, 100, 200, 400, 600 ppm ❖ Temperatures: 25 °C (electrochemical Test), 70 °C (weight loss) ❖ Immersion time: 72 h (weight loss) f) Results: Max IE: 83.70% (600 ppm, 25 °C, potentiodynamic polarization)	Limitations: No information about temperature and immersion time variations in electrochemical and weight loss experiments of corrosion inhibition Remarks: Vary temperature and immersion time	[55]
16	a) *N*-doped carbon dots from citric acid monohydrate and ethanolamine b) Media: HCl 0.1 M solution c) Metal/alloy: Q235 carbon steel d) Methods: Potentiodynamic polarization, EIS, weight loss, surface analysis (SEM and XPS) e) Parameters: ❖ Concentrations: 100, 300, 500 ppm ❖ Temperatures: 25, 30, 40, 60, 80 °C ❖ Immersion times: 1, 5, 10, 20, 30, 50, 70 h f) Results: Max IE: 89.98% (500 ppm, 25 °C, 1 h, EIS)	-	[56]
17	a) *N*-doped carbon dots from dopamine b) Media: HCl 0.1 M solution c) Metal/alloy: Q235 carbon steel d) Methods: Potentiodynamic polarization, EIS, weight loss, surface analysis (SEM and LSCM) e) Parameters: ❖ Concentrations: 50, 100, 200, 400 ppm ❖ Temperatures: room temperature, 25, 35, 45, 55 °C ❖ Immersion times: 6, 12, 24, 60 h f) Results: Max IE: 96.10% (400 ppm, room temperature, potentiodynamic polarization, 24 h)	-	[57]
18	a) *N*-doped carbon dots from citric acid and urea b) Media: H_2SO_4 0.5 M solution c) Metal/alloy: Carbon steel d) Methods: Potentiodynamic polarization, EIS, weight loss, surface analysis (SEM, XPS, AFM) e) Parameters: ❖ Concentrations: 10, 20, 25, 30 ppm ❖ Temperature: room temperature, 25 °C ❖ Immersion times: 1 and 2 h f) Results: Max IE: 97.80% (30 ppm, 25 °C, potentiodynamic polarization, 1 h)	Limitations: Constant temperature Remarks: Vary temperature	[51]

No	Details	Gap	Ref.
19	a) *N*-doped carbon dots from tryptophan b) Media: HCl 1.0 M solution c) Metal/alloy: Q235 carbon steel d) Methods: Potentiodynamic polarization, EIS, weight loss, surface analysis (SEM, LSCM, XPS) e) Parameters: ❖ Concentrations: 50, 100, 150, 200 ppm ❖ Temperature: 25 °C ❖ Immersion time: 24 h f) Results: Max IE: 96.00% (200 ppm, 25 °C, potentiodynamic polarization)	Limitations: Constant temperature and immersion time Remarks: Vary temperature and immersion time	[58]
20	a) *N*-doped carbon dots from citric acid and polyethyleneimine branched (PEI) b) Media: H_2SO_4 0.5 M solution c) Metal/alloy: Copper d) Methods: Potentiodynamic polarization, EIS, surface analysis (SEM, AFM, EDS, FTIR, Raman spectroscopy) e) Parameters: ❖ Concentrations: 0.2, 2, 50, 100 ppm ❖ Temperatures: 25, 35, 45 °C ❖ Immersion time: 40 min f) Results: Max IE: 96.10% (100 ppm, 25 °C, potentiodynamic polarization, 40 min)	Limitations: Constant immersion time Remarks: Vary immersion time	[59]
21	a) *N*-doped carbon dots from citric acid and *L*-serine b) Media: H_2SO_4 0.5 M solution c) Metal/alloy: Copper d) Methods: Potentiodynamic polarization, EIS, surface analysis (SEM, AFM, EDS) e) Parameters: ❖ Concentrations: 10, 25, 50, 100, 200 ppm ❖ Temperatures: 25, 35, 45 °C ❖ Immersion times: 0.5, 4, 8, 12, 24 h f) Results: Max IE: 98.5% (200 ppm, 25 °C, EIS, 24 h)	-	[60]
22	a) *N*,S-co-doped carbon dots from ammonium citrate and methionine b) Media: HCl 1.0 M solution c) Metal/alloy: Q235 carbon steel d) Methods: Potentiodynamic polarization, EIS, surface analysis (SEM, LSCM) e) Parameters: ❖ Concentrations: 50, 100, 150, 200 ppm ❖ Temperature: 25 °C ❖ Immersion times: 2, 6, 12, 24 h f) Results: Max IE: 98.00% (200 ppm, 25 °C, potentiodynamic polarization, 24 h)	Limitations: Constant temperature Remarks: Vary temperature	[61]
23	a) *N*-doped carbon dots from citric acid and ethylenediamine b) Media: HCl 1.0 M solution c) Metal/alloy: Q235 carbon steel d) Methods: Potentiodynamic polarization, EIS, surface analysis (SEM, XPS, AFM, contact Angle measurement) e) Parameters: ❖ Concentrations: 5, 10, 50, 100 ppm	Limitations: no information about temperature variation and immersion time Remarks: Vary temperature and immersion time	[46]

No		Details	Gap	Ref.
		❖ Temperature: 25 °C ❖ Immersion times: -		
	f)	Results: Max IE: 93.70% (100 ppm, 25 °C, EIS)		
24	a)	*N*-doped carbon quantum dots from folic acid and o-phenylenediamine	Limitations: No information about temperature variation and immersion time Remarks: Vary temperature and immersion time	[62]
	b)	Media: HCl 1.0 M solution		
	c)	Metal/alloy: Q235 carbon steel		
	d)	Methods: Potentiodynamic polarization, EIS, surface analysis (SEM, EDS, XPS, FTIR, AFM, contact Angle measurement)		
	e)	Parameters: ❖ Concentrations: 10, 50, 100, 150 ppm ❖ Temperature: 25 °C ❖ Immersion times: -		
	f)	Results: Max IE: 95.40% (150 ppm, 25 °C, EIS)		
25	a)	*N*-doped carbon quantum dots from 4-amino salicylic acid and *L*-histidine	Limitations: Constant temperature Remarks: Vary temperature	[63]
	b)	Media: HCl 1.0 M solution		
	c)	Metal/alloy: Q235 carbon steel		
	d)	Methods: Potentiodynamic polarization, EIS, weight loss, surface analysis (SEM, AFM)		
	e)	Parameters: ❖ Concentrations: 5, 10, 20, 50 ppm ❖ Temperature: 25 °C ❖ Immersion times: 12, 24, 36, 48, 60 h		
	f)	Results: Max IE: 93.50% (50 ppm, 25 °C, 20 h, weight loss)		
26	a)	*N*-doped carbon dots from malononitrile and urea		[64]
	b)	Media: HCl 15% solution	-	
	c)	Metal/alloy: Mild steel		
	d)	Methods: Potentiodynamic polarization, EIS, weight loss, surface analysis (SEM, XPS, AFM)		
	e)	Parameters: ❖ Concentrations: 15, 30, 50, 75, 100 ppm ❖ Temperature: 30, 40, 50, 60 °C ❖ Immersion times: 6, 12, 18, 24, 30, 36, 42, 48 h		
	f)	Results: Max IE: 97.90% (100 ppm, 30 °C, EIS)		
27	a)	*N*-doped carbon dots from malononitrile and 5-hydroxyisopthalic acid		[64]
	b)	Media: HCl 15% solution	-	
	c)	Metal/alloy: Mild steel		
	d)	Methods: weight loss, EIS, Potentiodynamic polarization, surface analysis (SEM, XPS, AFM)		
	e)	Parameters: ❖ Concentrations: 15, 30, 50, 75, 100 ppm ❖ Temperature: 30, 40, 50, 60 °C ❖ Immersion times: 6, 12, 18, 24, 30, 36, 42, 48 h		
	f)	Results: Max IE: 91.80% (150 ppm, 30 °C, EIS)		

spectrophotometers, respectively [14,40]. The chemical structure of CDs is also analyzed by Raman spectroscopy and X-ray diffractometry (XRD) [44-45]. Besides, XRD is used to determine the degree of crystallinity of obtained CDs [46]. Then, morphology/topography and particle/grain sizes are analyzed with scanning electron microscopy (SEM) [44,47], transmission electron microscopy (TEM) [14,47-48], scanning probe microscope (SPM) [44,49], and atomic force microscope (AFM) [4,23]. Furthermore, the chemical composition and bonding state on CDs are measured by X-ray photoelectron spectroscopy (XPS) [23,49-50]. The Zeta potential of CDs is measured by Zetasizer nano (ZS) [49]. Combinations of those methods are often conducted for better results. Meanwhile, the corrosion inhibition test is carried out by potentiodynamic polarization or Tafel test, electrochemical impedance spectroscopy (EIS), and weight loss methods. In this systematic literature review, carbon/mild steel, copper, and aluminium were used as metal objects in the corrosion experiments.

■ CARBON DOTS-BASED CORROSION INHIBITORS

Protector on Carbon/Mild Steel

Reduction of corrosion rate on the carbon/mild steel in hydrochloride acid using several doped CDs inhibitors has been reported. Nitrogen-doped carbon quantum dots (*N*-CQDs) that were produced from citric acid, urotropine, and diethylenetriamine as precursors are an example [14]. The synthesis process applied the microwave method for producing *N*-CQDs with sizes 4-10 nm. Analysis results from the EIS technique inform that the highest inhibition efficiency (*IE*) of *N*-CQDs toward carbon steel in 1 M HCl solution is 84.9% [14]. *N*-CQDs based-corrosion inhibitor has good performance at room temperature and higher temperatures. The other nitrogen-doped carbon dots (*N*-CDs) have been synthesized with 4-aminosalicylic acid as a precursor through the solvothermal method [40] and a combination of citric acid and urea as precursors through the hydrothermal method [51]. *N*-CDs from 4-aminosalicylic acid approximately have average sizes and heights of 3 nm and 2–4 nm, respectively, whereas *N*-CDs from citric acid and urea have a spherical form with an average size of 10–14 nm. Corrosion tests using carbon steel in 1 M HCl and 0.5 M H_2SO_4 solutions reveal inhibition efficiencies (IE) increased by increasing the concentration of *N*-CDs, respectively. The maximum values of inhibition efficiencies are stagnant after reactions among the inhibitor molecules and iron atoms/ions on the carbon steel surface reach equilibrium. *N*-CDs from 4-aminosalicylic acid have better performance for inhibiting corrosion reaction in HCl solution than *N*-CQDs from citric acid, urotropine, and diethylenetriamine at the same temperature. Its inhibition efficiency > 95% at lower concentration. This may relate to the size of synthesized CDs which affects contact surface area. Smaller materials have larger surface area for covering steel surface from corrosion species, thus increasing inhibition efficiency.

Nyquist plots from EIS analysis describe the similar shape of the semicircle curves due to no changes in the electrochemical process for inhibited and uninhibited solutions. Weak interactions between metal atoms/ions and inhibitor molecules are the main reason [40]. These interactions refer to inhibition processes of inhibitors on the interface area, such as active site blocking, geometric blocking, and electrocatalytic resisting [52]. Meanwhile, the polarization curves in the potentiodynamic polarization measurements relatively shift to more negative potential after increasing inhibitor concentrations. Therefore, *N*-CDs were suggested as a cathodic-type inhibitor. In this condition, the cathodic current density decreases more significantly than the anodic current density. Protection on one site (anode or cathode) is enough to stop the whole electrochemical reaction.

Other studies also reported manufacturing corrosion inhibitor-based nitrogen-carbon dots (*N*-CDs) from ammonium citrate as a precursor through pyrolysis [45,49]. The products are water-soluble. Hence, those CDs were different from other CDs sources because the preparation did not need initiated dispersion with organic solvents like diethyl ether, ethanol, or acetone. The increase in concentrations was followed by increasing open circuit potential and

inhibition efficiency. *N*-CDs based-inhibitors from ammonium citrate are classified as mixed-type inhibitors, predominantly anodic inhibitors. Both of these carbon dots generally have a similar structure. In addition, the type of metal and electrolyte/corrosive solution is also not different. Hence, the difference in inhibition type may be affected by variations in temperatures and reaction times during the synthesis process of carbon dots. Cen et al. [4] and Luo et al. [61] reported other types of inhibitor-based carbon dots. Not only nitrogen, but they also inserted sulphur elements to generate *N,S*-co-doped carbon dots. The precursors are the mixtures of aminosalicylic acid-thiourea and ammonium citrate-methionine carried out by the hydrothermal method. These nanomaterials are effectively applied in CO_2-saturated 3.5% NaCl and HCl 1 M solutions. The inhibition efficiencies of these *N,S*-CDs are high even at very low concentrations. *N,S*-CDs have been significantly reduced corrosion current density due to their functional groups and supported by nanoparticle character [4]. The performance of *N*-CDs and *N,S*-CDs to mitigate corrosion reaction on mild steel had been compared [48]. As a result, *N,S*-CDs have slightly higher inhibition efficiency than *N*-CDs. The presence of an additional element (sulphur) in CDs generates stronger interaction with the mild steel surface [65].

Functionalized carbon dots are basically similar to *N*-CDs. Hence, there are 18 types of *N*-CDs from different natural sources and different synthesized methods. Their performance as corrosion inhibitors on carbon steel is almost similar, and the inhibition efficiency increases by increasing concentrations. However, each *N*-CDs has a different performance depending on its structure and character. Utilization of amino acids as one of the precursors generated effective CDs-based corrosion inhibitors (IE > 90%). It relates to the role of carboxyl and amine groups as active sites in the coordination reaction/adsorption process. Generally, *N*-CDs are tested in an acidic solution like HCl or H_2SO_4. Apart from reasons of need, this may be caused by the perfect solubility property of the *N*-CDs in acidic solution, which was required for optimum performance as an inhibitor. Only *N,S*-CDs can be applied in NaCl solution, but this is also along with CO_2 sparging. The existence of CO_2 will generate a slightly acid solution from the carbonic acid formation [18,66]. Details and research gaps on several types of carbon dots-based corrosion inhibitors from various precursors are summarized in Table 1. It was sorted based on publication time. Table 1 explains that synthesized carbon dots from various organic sources effectively inhibit corrosion reactions in different metals and media. Immersion time variations commonly refer to the weight loss method. The inhibition efficiencies are generally more than 90%. Meanwhile, all types of *N,S*-CDs have a better protective ability. This corresponds to additional sulphur atoms as additional active sites which adhere to the metal surface.

Protector on Copper Metal/Alloy

The corrosion rate on copper metal/alloy in sodium chloride solution can be controlled by original carbon dots from durian juice [53]. Fluorescence property and intensity were displayed through blue light emission at 365 nm of wavelength in UV light. The hydrophilic character is needed when using brine or neutral solutions as aggressive media. Consequently, synthesized CDs must have good solubility in water. Its inhibition ability comes from the activity of sulphur-based compounds, for instance, short-chain alkanethiols, hydrogen sulfide, and ethyl (2S)-2-methyl butanoate [67]. Besides, the carboxylate groups make a difference in dipole moment and produce significant intermolecular attractions between adsorbed inhibitor molecules and copper ions on the copper/solution interface. These CDs are classified as cathodic-type inhibitors and have maximum inhibition efficiency of up to 85.84% after being measured by the potentiodynamic polarization technique [53].

Furthermore, the inhibition of corrosion on copper metal in an H_2SO_4 solution can be conducted by adding *N*-doped carbon dots from 4-aminosalicylic acid as a corrosion inhibitor [22]. These CDs were synthesized by the solvothermal method. The presence of heteroatoms and double bonds in its structure is the main factor for copper protection. It was categorized as a mixed inhibitor which tends predominantly as a cathodic inhibitor. The adsorption mechanism obeys the

Langmuir adsorption isotherm that the interaction consists of physical and chemical adsorption. Then, *N*-doped CDs were synthesized from citric acid as a carbon source doped with nitrogen from polyethyleneimine branched [59] or *L*-serine [60]. These *N*-CDs are significantly effective in inhibiting corrosion reaction on copper by the presence of H_2SO_4 solution. The obtained inhibition efficiency is above 95%. Both of them obey Langmuir adsorption isotherm and are classified as mixed-type inhibitors. Meanwhile, the straight-tailed line in Nyquist curves after impedance measurements represents Warburg impedance. This corresponds to copper dissolution, which is affected by the diffusion and charge transfer process [59]. Adsorption *N*-CDs on a metal surface is described by the Bode plot. The indicator is the increase of impedance modulus and maximum phase angle after increasing inhibitor content.

Protector on Aluminium Metal/Alloy

In addition to carbon steel and copper, aluminium metal/alloy also can be protected by carbon dots-based inhibitors. Cen et al. [23] disclosed that nitrogen and sulphur co-doped carbon dots (*N,S*-CDs) are an effective inhibitor to retard corrosion rate on aluminium alloy in acid solution (0.1 M HCl). These *N,S*-CDs only dispersed in an ethanol solution, so the dispersed solution must have been oscillated before being used. Maximum efficiency from several corrosion analytical methods is 85% at a very low concentration (5 $mg.L^{-1}$). Proposed inhibition mechanisms of *N,S*-CDs are via diffusion and agglomeration on aluminium alloy surfaces accompanied by protective film formation on the surface. This thin film is formed by the interaction between functional groups or heteroatoms in *N,S*-CDs molecules with aluminium ions on the surface. Electrochemical reactions in anode and cathode are also inhibited by this protective film [23]. Nevertheless, the presence of ethanol solution may affect the performance of the inhibitor even though using ethanol-HCl mixture is used as a blank solution. It can support or compete with *N,S*-CDs to contact and adsorb on the aluminium surface. *N,S*-CDs were classified as mixed-type inhibitors, predominantly cathodic inhibitors based on the corrosion potential movement (leading to the negative direction) [68]. Furthermore, the protective thin film on the metal surface is confirmed through surface analysis.

■ SURFACE ANALYSIS

Surface analysis is carried out to observe the condition of metal surfaces in contact with the surrounding environment. This analysis investigates the structure, reactivity, and corrosion resistance of a testing metal in an aggressive solution with and without corrosion inhibitors. Metal specimens should be polished, cleaned, and dried before being analyzed to obtain proper image/spectra. There are several methods for analyzing the state of metal surfaces in corrosion experiments, for instance, energy-dispersive X-ray spectroscopy (EDS), Fourier transform infrared spectroscopy (FTIR), X-ray photoelectron spectroscopy (XPS), Raman spectroscopy, atomic force microscope (AFM), laser scanning confocal microscopes (LSCM), inverted fluorescence microscope (IFM), surface profiler, and contact angle meter (CAM). The research schematic with respect to surface analysis in CDs-based corrosion inhibitor experiments is displayed in Fig. 4.

Analysis results of two and three-dimension metal/alloy morphologies after the corrosion test describe the difference in physical appearance among metals that are immersed in the blank solution and the solution with various concentrations of inhibitor. The unprotected metals have been seriously broken with the presence of holes, cracks, and roughness on their surface. In contrast, protected surface metals are seen as flatter or smoother. These roughness levels depend on the concentration of the inhibitor, temperature, aggressiveness of the solution, and immersion time [44]. In addition, large and deep pit sizes in a metal surface without inhibitors can be displayed.

XPS analysis is conducted to understand the adsorption type and chemical nature of protective film on the metal surface [51]. The amount of adsorbed CDs-based inhibitors increases with the prolongation of the immersion time [23]. This adsorption process depends on diffusion rate and interactions between inhibitor molecules and metal atoms/ions. The protective film

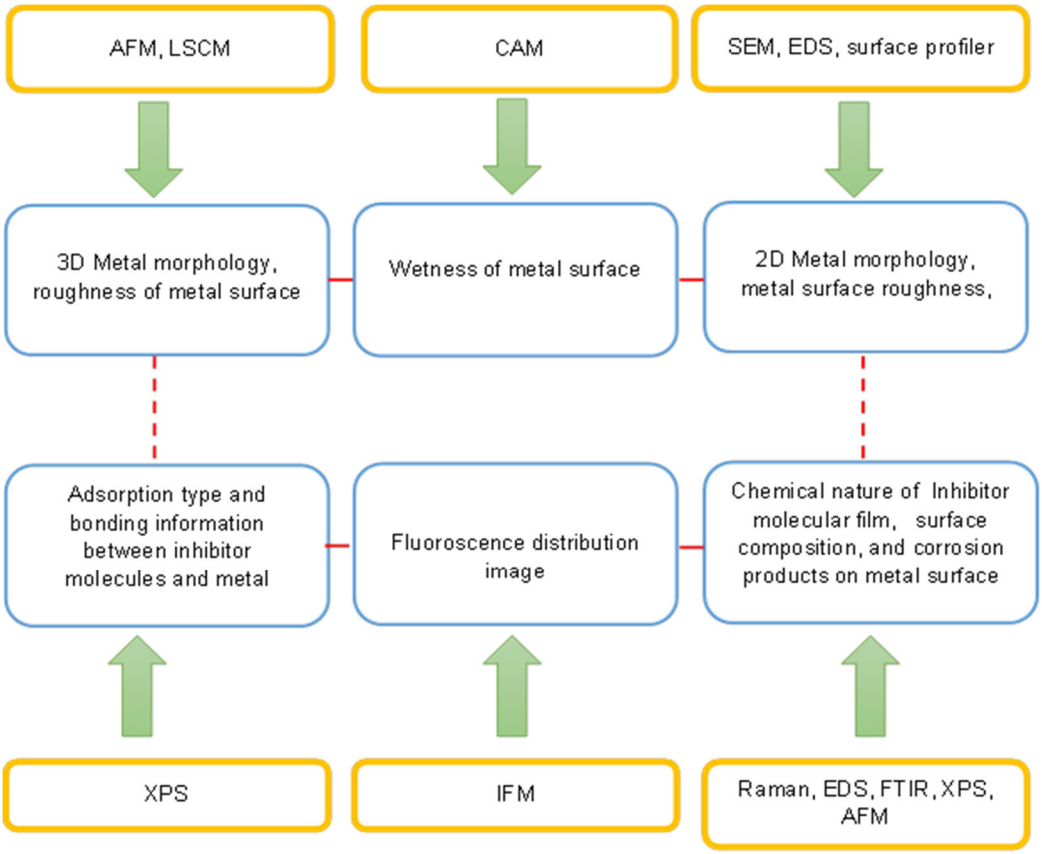

Fig 4. Research schematic for surface analysis in CDs-based corrosion inhibitor experiments

formation on the metal surface is incomplete in a shorter period. EDS spectra of metal with *N*-CDs as corrosion inhibitors will display the presence/increase in C and N peaks to confirm inhibitor adsorption on the metal surface. This is accompanied by a reduction of peak intensity chlorin element in HCl solution or sulphur element in H_2SO_4 solution. Another parameter that determines the effectiveness of CDs-based corrosion inhibitors is the wetness of the metal surface. The wetness level is determined by contact angle measurement. Thin film from adsorbed inhibitor will raise the contact angle of metal in corrosive media. It corresponds to higher hydrophobicity of metal surface by the presence of inhibitor on the surface [62].

■ ADSORPTION AND/OR INHIBITION MECHANISM

XPS analysis is a method to ensure the adsorption of inhibitors on the metal surface. For *N*-CDs, XPS spectra of protected steel will contain nitrogen peaks. It also confirms adsorption types among metal ions and inhibitor molecules [49]. The power of adsorption can be determined by the value of the equilibrium constant (K_{ads}). A higher value of K_{ads} suggests stronger adsorption of a corrosion inhibitor. Besides that, the adsorption type is known from the value of adsorption-free energy ($\Delta G°_{ads}$) and/or enthalpy of adsorption (ΔH_{ads}). When the value of $\Delta G°_{ads} \geq -20$ kJ.mol^{-1}, an inhibitor is physically adsorbed onto the metal surface. Whereas, If the $\Delta G°_{ads} \leq -40$ kJ.mol^{-1}, the adsorption type of inhibitor is chemical adsorption [69]. Then, in the range of −20 and −40 kJ.mol^{-1}, an inhibitor is both physically and chemically adsorbed on the metal surface [40]. From $\Delta G°_{ads}$ values, *N*-CDs as well as *N,S*-CDs were physically and chemically adsorbed on the carbon/mild steel-solution interface [44,49,61]. Annotations of adsorption energy, adsorption type, adsorption isotherm, and type of inhibitor in various metals and media are listed in Table 2. Meanwhile, adsorption of *N,S*-CDs molecules on the aluminium surface mostly via coordination

bonds between functional groups (heterocyclic, carboxyl, hydroxyl) and aluminium ions [70-71]. A few chemisorptions are formed via covalent bonds among heteroatoms in *N,S*-CDs with aluminium atoms on the surface [72]. Chelation reactions between the mixture of CDs and metal ions that refer to chemical adsorption can be determined by conductivity and fluorescence intensity [23].

CDs-based corrosion inhibitors on carbon/mild steel, copper, and aluminium have been fitted with some adsorption isotherm types such as Langmuir, Freundlich, Temkin, Frumkin, etc. All synthesized *N*-CDs with different precursors have the degree of fitting, R^2 value ≥ 0.99 in the relation of C and C/θ. This indicates that the adsorption of inhibitors on the carbon steel and copper surfaces obeyed the Langmuir adsorption model [14,22, 40,44,49,63]. In this condition, carbon dots materials occupy specific sites and form a monolayer protector. A similar case also occurs for adsorption isotherm of *N,S*-CDs on carbon/mild steel that follows the Langmuir adsorption model. However, *N,S*-doped carbon dots from aminosalicylic and thiourea tend to accumulate on the aluminium surface and form a multilayer protector [23]. This indicates that the adsorption of *N,S*-CDs to aluminium surface theoretically does not obey Langmuir adsorption isotherm.

Corrosion occurs due to electrochemical reactions on the metal sites. These reactions generate either hydrogen gas (H_2) in acidic solutions without oxygen, H_2O in acidic solutions with oxygen, or hydroxide ions (OH^-) in neutral or basic solutions (Fig. 1). Corrosion inhibitors act to retard reaction on the cathode only (cathodic inhibitors) [73], on the anode (anodic inhibitors) [74], or both (mixed inhibitors) [75]. Anodic inhibitors need minimum concentrations for effectively inhibitive performance because very low concentrations can accelerate corrosion reaction [76]. On the other hand, cathodic inhibitors do not have a corrosion effect at all ranges of concentration [77]. These inhibitors prevent reaction on the cathodic site through disturbing electron travel from anode to cathode [78]. Furthermore, the mixed inhibitor can protect anode and cathode sites through adsorption on the metal surface, forming the protective layer and reducing electrical conductivity after substituting water molecules [79]. Polarization curves for protected and unprotected metals in cathodic and/or anodic sides of a metal/alloy which mutual parallel suggests no inhibition effect on the cathode and/or anode reactions [80]. Meanwhile, the classification of corrosion inhibitors (anodic, cathodic, and mixed-type) can also be determined through corrosion potential shifted based on the Tafel test as follows:

- Corrosion potential shifts to a positive direction and/or less negative value more than 85 mV: anodic inhibitor [68]
- Corrosion potential shifts to a negative direction and/or more negative value of more than 85 mV: cathodic inhibitor [68]
- Corrosion potential shifts to a positive/negative direction and less/more negative value less than 85 mV: mixed inhibitor [81].

Table 1 displays almost all CDs-based corrosion inhibitors are classified as mixed-type inhibitors that are physically and chemically adsorbed on metal surfaces. Inhibition mechanisms of most organic inhibitors on the metallic surface are almost considered similar. They can form a protective layer after physical or chemical interactions between metal or metal ions and heteroatoms and/or non-saturated bonds in their functional groups [69]. The power of adsorption depends on polarizability, the presence of π orbital, and electron density in the polar groups as the adsorbing agent [82]. Aluminium metal has the vacant d-orbital in the outer surface layer. Thereby, chemical interactions or covalent bonds among heteroatoms and atoms on the metal surface are scanty [72]. On the other hand, the chelating complexes of Al^{3+} are more easily formed by coordination with functional groups like hydroxyl, carboxyl, and heterocyclic groups [70-71].

■ KINETIC AND THERMODYNAMIC STUDY

In this part, the kinetic and thermodynamic parameters of the corroded and protected system are studied. These parameters are commonly achieved from gravimetric or weight loss analysis. Kinetics parameters for several carbon dots-based inhibitors in various metals

Table 2. Annotations of adsorption energy, adsorption type, adsorption isotherm, and type of inhibitor in various metals and media

	Corrosion inhibitor	Adsorption energy and adsorption type	Adsorption Isotherm	Type of Inhibitor	Ref.
1)	*N*-doped carbon dots from Aminosalicylic acid (ASA)	$\Delta G^{o}_{ads} = -34.6$ kJ.mol^{-1} Chemisorption and physisorption	Langmuir adsorption isotherm	Mixed type inhibitor, a predominantly cathodic inhibitor	[40]
2)	Carbon dots from Durian Juice	-	-	Anodic inhibitor	[53]
3)	*N*-doped carbon dots from p-phenylenediamine (p-PD) and o-phenylenediamine (o-PD)	$\Delta G^{o}_{ads} = -33.19$ kJ.mol^{-1} (p-PD) and $\Delta G^{o}_{ads} = -27.83$ kJ.mol^{-1} (o-PD) Chemisorption and physisorption	Langmuir adsorption isotherm	Mixed type inhibitor, a predominantly anodic inhibitor	[47]
4)	*N*-doped carbon dots from citric acid, diethylenetriamine, and urotropine	$\Delta G^{o}_{ads} = -25.42$ kJ.mol^{-1} Chemisorption and physisorption	Langmuir adsorption isotherm	Mixed type inhibitor, a predominantly cathodic inhibitor	[14]
5)	*N,S*- co-doped carbon dots from aminosalicylic and thiourea	- Chemisorption and physisorption	-	Mixed type inhibitor, a predominantly cathodic inhibitor	[23]
6)	*N,S*- co-doped carbon dots from 4-Aminosalicylic acid and thiourea	- Chemisorption and physisorption	-	Mixed type inhibitor, a predominantly anodic inhibitor	[4]
7)	Functionalized carbon dots from citric acid, (1-(3-dimethyl aminopropyl)-3-ethyl carbodiimide hydrochloride, N-carboxysuccinimide, N-(3-aminopropyl) imidazole, triethylamine	$\Delta G^{o}_{ads} = -30.04$ kJ.mol^{-1} Chemisorption and physisorption	Langmuir adsorption isotherm	Mixed type inhibitor, a predominantly anodic inhibitor	[54]
8)	Functionalized carbon dots from imidazole ionic liquids and citric acid	$\Delta G^{o}_{ads} = -29.23$ kJ.mol^{-1} in 1 M HCl and $\Delta G^{o}_{ads} = -25.45$ kJ.mol^{-1} in 3.5 wt.% NaCl Chemisorption and physisorption	Langmuir adsorption isotherm	Mixed type inhibitor, a predominantly cathodic inhibitor	[50]
9)	*N*-doped carbon dots from 4-Aminosalicylic acid	$\Delta G^{o}_{ads} = -34.00$ kJ.mol^{-1} Chemisorption and physisorption	Langmuir adsorption isotherm	Mixed type inhibitor, a predominantly cathodic inhibitor	[22]
10)	*N*-doped carbon dots from ammonium citrate	$\Delta G^{o}_{ads} = -26.94$ kJ.mol^{-1} Chemisorption and physisorption	Langmuir adsorption isotherm	Mixed type inhibitor, a predominantly anodic inhibitor	[49]
11)	*N*-doped carbon dots from methacrylic acid and n-butylamine	$\Delta G^{o}_{ads} = -28.29$ kJ.mol^{-1} Chemisorption and physisorption	Langmuir adsorption isotherm	Mixed type inhibitor, a predominantly anodic inhibitor	[44]

12)	*N,S*-co-doped carbon dots from thiourea and diethylene triamine	$\Delta G^{o}_{ads} = -22.93$ kJ.mol^{-1} $\Delta H_{ads} = -14.66$ kJ.mol^{-1} Physisorption	Langmuir adsorption isotherm	Mixed type inhibitor, a predominantly cathodic inhibitor	[48]
13)	*N*-doped carbon dots from urea and diethylene triamine	$\Delta G^{o}_{ads} = -22.76$ kJ.mol^{-1} $\Delta H_{ads} = -14.08$ kJ.mol^{-1} Physisorption	Langmuir adsorption isotherm	Mixed type inhibitor	[48]
14)	*N*-doped carbon dots from ammonium citrate	$\Delta G^{o}_{ads} = -26.94$ kJ.mol^{-1} Chemisorption and physisorption	Langmuir adsorption isotherm	Mixed type inhibitor, a predominantly anodic inhibitor	[45]
15)	*N*-doped carbon quantum dots from disodium EDTA, sulfamic acid, and urotropine salt	-	-	Mixed type inhibitor, a predominantly cathodic inhibitor	[55]
16)	*N*-doped carbon dots from citric acid monohydrate and ethanolamine	$\Delta G^{o}_{ads} = -26.65$ kJ.mol^{-1} Chemisorption and physisorption	Langmuir adsorption isotherm	Mixed type inhibitor, a predominantly anodic inhibitor	[56]
17)	*N*-doped carbon dots from dopamine	$\Delta G^{o}_{ads} = -28.10$ kJ.mol^{-1} Chemisorption and physisorption	Langmuir adsorption isotherm	Mixed type inhibitor, a predominantly anodic inhibitor	[57]
18)	*N*-doped carbon dots from citric acid and urea	$\Delta G^{o}_{ads} = -30.00$ kJ.mol^{-1} Chemisorption and physisorption	Langmuir adsorption isotherm	Mixed type inhibitor, a predominantly cathodic inhibitor	[51]
19)	*N*-doped carbon dots from tryptophan	$\Delta G^{o}_{ads} = -29.37$ kJ.mol^{-1} Chemisorption and physisorption	Langmuir adsorption isotherm	Mixed type inhibitor, a predominantly anodic inhibitor	[58]
20)	*N*-doped carbon dots from citric acid and polyethyleneimine branched (PEI)	$\Delta G^{o}_{ads} = -33.39$ kJ.mol^{-1} Chemisorption and physisorption	Langmuir adsorption isotherm	Mixed type inhibitor, a predominantly cathodic inhibitor	[59]
21)	*N*-doped carbon dots from citric acid and *L*-serine	$\Delta G^{o}_{ads} = -27.25$ kJ.mol^{-1} Chemisorption and physisorption	Langmuir adsorption isotherm	Mixed type inhibitor, a predominantly cathodic inhibitor	[60]
22)	*N,S*- co-doped carbon dots from ammonium citrate and methionine	$\Delta G^{o}_{ads} = -29.75$ kJ.mol^{-1} Chemisorption and physisorption	Langmuir adsorption isotherm	Mixed type inhibitor	[61]
23)	*N*-doped carbon dots from citric acid and ethylenediamine	$\Delta G^{o}_{ads} = -34.43$ kJ.mol^{-1} Chemisorption and physisorption	Langmuir adsorption isotherm	Mixed type inhibitor, a predominantly anodic inhibitor	[46]
24)	*N*-doped carbon quantum dots from folic acid and o-phenylenediamine	$\Delta G^{o}_{ads} = -34.41$ kJ.mol^{-1} Chemisorption and physisorption	Langmuir adsorption isotherm	Mixed type inhibitor, a predominantly anodic inhibitor	[62]

25)	*N*-doped carbon quantum dots from 4-amino salicylic acid and *L*-histidine	$\Delta G^{o}_{ads} = -33.63$ kJ.mol^{-1} Chemisorption and physisorption	Langmuir adsorption isotherm	Mixed type inhibitor, a predominantly cathodic inhibitor	[63]
26)	*N*-doped carbon dots from malononitrile and urea	$\Delta G^{o}_{ads} = -23.22$ kJ.mol^{-1} Chemisorption and physisorption	Langmuir adsorption isotherm	Mixed type inhibitor, a predominantly anodic inhibitor	[64]
27)	*N*-doped carbon dots from malononitrile and 5-hydroxy isophthalic acid	$\Delta G^{o}_{ads} = -23.07$ kJ.mol^{-1} Chemisorption and physisorption	Langmuir adsorption isotherm	Mixed type inhibitor	[64]

- : Not mentioned

and media are listed in Table 3. The activation energy (E_a) of the corrosion process is calculated from the Arrhenius equation (Eq. 1) [48]. Besides that, activation entropy ΔS^* and enthalpy ΔH^* are determined transition formulas (Eq. 2) [56].

$$\log C_R = \frac{E_a}{2.303RT} + \log A \quad (1)$$

$$C_R = \frac{RT}{NH} e^{\frac{\Delta S^*}{R}} e^{\frac{-\Delta H^*}{RT}} \quad (2)$$

where C_R is the corrosion rate, E_a is the activation energy, T is temperature, *A* is the pre-exponential constant, and R is the universal molar constant of gas. Corrosion rate (C_R) can also be written as corrosion current density (I_{corr}). The activation energy (E_a) of the system gives information about the ease with which corrosion reactions occur. Corrosion inhibitors that retard corrosion rate through movement reduction of mass and charge on the interface area will generate higher activation energy of the system [56]. On the ideal condition, the value of E_a is almost similar to ΔH^* [56]. *N*-doped carbon dots from citric acid monohydrate and ethanolamine have positive values of E_a and ΔH^*. This corresponds to the endothermic reaction of metal dissolution. Otherwise, a negative value of this parameter relates to the exothermic reaction. This result is similar to inhibitors from *N,S*-co-doped carbon dots from thiourea-diethylene triamine, and urea-diethylene triamine. The presence of these inhibitors increases both E_a and ΔH^*. Corrosion reaction is inhibited in the positive and higher enthalpy value. Thereby higher energy is required to continue the corrosion process. Meanwhile, the value of activation entropy indicates the irregularity degree of the system due to corrosion reaction. A negative value in ΔS^* corresponds to the formation of an activated complex on the surface, which decreases the disorder of the system and vice versa for a condition with a positive value in ΔS^* [83]. High values in E_a and ΔH^* (up to $\pm$ 80 kJ.mol^{-1}) even generate positive ΔS^*. This condition may be caused by the extent of the inhibitor coverage on the metal surface that creates irregularity. The nature of the inhibitor molecules and their changes on the metal surface can also be calculated computationally.

Table 3. Kinetics parameters for carbon dots-based inhibitors in various metals and media.

	Corrosion inhibitor	Max E_a (kJ.mol^{-1})	Max ΔH^* (kJ.mol^{-1})	Max ΔS^* (J.mol^{-1}K^{-1})	Ref.
1)	*N,S*-co-doped carbon dots from thiourea and diethylene triamine	84.47	81.83	28.47	[48]
2)	*N*-doped carbon dots from urea and diethylene triamine	65.50	62.86	–26.24	[48]
3)	*N*-doped carbon dots from citric acid monohydrate and ethanolamine	32.17	29.29	–115.26	[56]
4)	*N*-doped carbon dots from dopamine	47.94	45.34	–90.62	[57]
5)	*N*-doped carbon dots from citric acid and *L*-serine	49.17	49.61	–81.26	[60]
6)	*N*-doped carbon dots from malononitrile and urea	80.97	78.33	17.0	[64]
7)	*N*-doped carbon dots from malononitrile and 5-hydroxyisopthalic acid	62.87	60.23	–34.25	[64]

■ THE QUANTUM COMPUTATIONAL CHEMISTRY STUDY

Substantial parameters of the computational study in the use of carbon dots-based corrosion inhibitors encompass the optimized structure of CDs-based corrosion inhibitors, Energy of Highest Occupied Molecular Orbital (E_{HOMO}), Energy of Lowest Unoccupied Molecular Orbital (E_{LUMO}), energy gap (ΔE), dipole moment (μ), and interaction/adsorption energy. These parameters are calculated from the quantum chemical calculations. A higher value of E_{HOMO} indicates the convenience of CDs for donating electrons to protect metal/alloy. In comparison, lower E_{LUMO} relates to the ability of inhibitor molecules to accept electrons [84]. Thereby, both of them inform how the electron transfer occurs between CDs and metals. Adsorption capacity and polarity of the inhibitor are determined by ΔE and μ, respectively. Larger adsorption capacity and higher reactivity are obtained on the lower ΔE. Then, the higher polarity of CDs than water implies the replacement of water molecules on the metal surface by CDs [63]. Furthermore, there is an interaction/adsorption energy parameter that determines adsorption strength as well as corrosion inhibition ability of CDs. Computational chemistry study also can explain inhibition mechanism based on the mentioned parameters through density functional theory. Electron density of both HOMO and LUMO is distributed in active sites of the CDs molecules. These active sites play a role in center adsorption in aromatic rings and/or other functional groups [84].

■ SIGNIFICANCE OF CARBON DOTS-BASED CORROSION INHIBITOR

Protection metal from corrosion continues to be developed through various studies. The utilization of corrosion inhibitors is an option for many researchers due to ease in the synthesis process, low cost, and effectiveness. Various substances have been tested as corrosion inhibitors in various metals and corrosive solutions. Most of them showed very high inhibition efficiency, which is very promising to be applied in the oil and gas industries. However, attention to environmental safety obliges the use of natural substances and minimizes the usage of chemicals. Several natural compounds commonly used as corrosion inhibitors and safety for the environment are chitosan and its derivates, amino acids, imidazoles, modified starch, etc. [85-89]. Moreover, expired drugs are another choice as corrosion inhibitors [90-91]. Carbon dots are just beginning to be developed as corrosion inhibitors. It has been previously used for many applications by taking advantage of its properties, but information about the direct application of carbon dots-based corrosion inhibitors in the industry has not been informed.

The application of corrosion inhibitors, including carbon dots-based corrosion inhibitors, was mostly aimed at the petroleum industry to protect the pipeline. Carbon steel is generally used as a pipeline base material. Thereby, carbon steel is used as a corrosion object. Whereas corrosion inhibitors in aluminium and copper are utilized when cleaning or pickling those metals with acid solutions. In this process, corrosion inhibitors are mixed with an acid solution to retard further corrosion reactions. CDs-based corrosion inhibitor also provides information about the effect of material size for inhibition activity besides molecular structure. Meanwhile, there are several limitations of carbon dots-based corrosion inhibitors that must be fixed to obtain superior corrosion inhibitors, for example.

- Several carbon dots-based corrosion inhibitors are not water-soluble. Thus, they must be dissolved in an organic solvent.
- Conventional inhibitors are mostly composed of tiny molecules. These inhibitors can rapidly diffuse and interact with the metal matrix on the metal surface to make a protective film. Whereas adsorption of nanomaterial was relatively slower in aqueous solution [4]. Hence, the study of material size effect on adsorption rate can be considered.

■ CONCLUSION AND FUTURE PROSPECTS

Carbon dots-based corrosion inhibitors and their derivates are potential substances for preventing the corrosion process in various metals and media. The inhibition efficiency of carbon dots on the metals reported reaches ±90%. This value informs that carbon

dots are effective substances as corrosion inhibitors. It has almost similar effectivity to conventional inhibitors. Synthesized CDs-based corrosion inhibitors work effectively in different metals (steel, copper, aluminium) and media (acid, neutral, and CO_2 saturated solutions). Several modifications to the carbon dots can be conducted to increase both their performance stability and the inhibition efficiency up to 100%. Generally, carbon dots-based corrosion inhibitors were tested in HCl solution. Thus, other types of electrolyte/corrosive solutions such as NaCl, H_2SO_4, and saturated CO_2 solutions may be used for further experiments. Besides that, scaling problems in industries become another challenge for researchers. Scaling can be prevented or reduced by adding inorganic acid solutions. However, acceleration of corrosion reaction also occurs simultaneously. This opens the chance to create CDs with double functions as corrosion and scale inhibitors. A compound with the ability as a corrosion and scale inhibitor can reduce the utilization of inorganic acid solutions. The main requirements for scale inhibitors are water solubility and the presence of functional groups as chelating agents. The synthesis of carbon dots-based green corrosion inhibitors and the utilization of appropriate methods were needed due to environmental safety is recently concerned. Hence, the use of organic solvent and other poisonous chemicals has been restricted. Meanwhile, the durability of adsorbed inhibitors on the metal surface toward mechanical shocks has not been tested. In comparison, the actual condition of the flowing fluids on the pipeline is dynamic. Therefore, corrosion tests using wheel test corrosion test can be conducted to obtain information about this aspect. Table 1 and Fig. 3 show CDs can be synthesized from several types of amino acids and other substances like ammonium citrate, citric acid, or 4-amino salicylic. Thereby, synthesis and evaluation of CDs-based corrosion inhibitors from other amino acids are possible to be carried out. Remarks in Table 1 also can be considered for further studies.

■ REFERENCES

[1] Stalheim, D., 2011, Metallurgical optimization of microalloyed steels for oil and gas transmission pipelines, *Proceedings of 6th International Conference on High Strength Low Alloy Steels (HSLA Steels 2011)*, Chinese Society for Metals, Beijing, China, May 31 – June 2, 2011.

[2] Adewuyi, A., Göpfert, A., and Wolff, T., 2014, Succinyl amide gemini surfactant from *Adenopus breviflorus* seed oil: A potential corrosion inhibitor of mild steel in acidic medium, *Ind. Crops Prod.*, 52, 439–449.

[3] Yilmaz, N., Fitoz, A., Ergun, Ü., and Emregül, K.C., 2016, A combined electrochemical and theoretical study into the effect of 2-((thiazole-2-ylimino)methyl)phenol as a corrosion inhibitor for mild steel in a highly acidic environment, *Corros. Sci.*, 111, 110–120.

[4] Cen, H., Chen, Z., and Guo, X., 2019, *N,S*-co-doped carbon dots as effective corrosion inhibitor for carbon steel in CO_2-saturated 3.5% NaCl solution, *J. Taiwan Inst. Chem. Eng.*, 99, 224–238.

[5] Kadry, S., 2008, Corrosion analysis of stainless steel, *Eur. J. Sci. Res.*, 22 (4), 508–516.

[6] Patel, A.S., Panchal, V.A., Mudaliar, G.V., and Shah, N.K., 2013, Impedance spectroscopic study of corrosion inhibition of Al-Pure by organic Schiff base in hydrochloric acid, *J. Saudi Chem. Soc.*, 17 (1), 53–59.

[7] Anbarasi, C.M., and Divya, G., 2017, A Green approach to corrosion inhibition of aluminium in acid medium using Azwain seed extract, *Mater. Today: Proc.*, 4 (4), 5190–5200.

[8] Lopez-Garrity, O., and Frankel, G.S., 2014, Corrosion inhibition of aluminum alloy 2024-T3 by sodium molybdate, *J. Electrochem. Soc.*, 161 (3), C95–C106.

[9] Ambat, R., and Dwarakadasa, E.S., 1994, Studies on the influence of chloride ion and pH on the electrochemical behaviour of aluminium alloys 8090 and 2014, *J. Appl. Electrochem.*, 24 (9), 911–916.

[10] Sequeira, C.A.C., 2011, "Copper and Copper Alloys" in *Uhlig's Corrosion Handbook*, 3rd Ed., Eds. Revie, R.W., John Wiley & Sons, Inc. USA, 757–785.

[11] Huang, H., Wang, Z., Gong, Y., Gao, F., Luo, Z., Zhang, S., and Li, H., 2017, Water soluble corrosion

inhibitors for copper in 3.5 wt% sodium chloride solution, *Corros. Sci.*, 123, 339–350.

[12] Antonijević, M.M., Milić, S.M., and Petrović, M.B., 2009, Films formed on copper surface in chloride media in the presence of azoles, *Corros. Sci.*, 51 (6), 1228–1237.

[13] Pahuja, P., Dahiya, S., and Lata, S., 2018, A review on herbal drugs as corrosion inhibitor for low alloy steel, *BMIET J. Sci. Technol. Manage.*, 2 (1), 7–19.

[14] Lv, J., Fu, L., Zeng, B., Tang, M., and Li, J., 2019, Synthesis and Acidizing corrosion inhibition performance of *N*-doped carbon quantum dots, *Russ. J. Appl. Chem.*, 92 (6), 848–856.

[15] Usman, B.J., and Ali, S.A., 2018, Carbon dioxide corrosion inhibitors: A review, *Arabian J. Sci. Eng.*, 43 (1), 1–22.

[16] Umoren, S.A., AlAhmary, A.A., Gasem, Z.M., and Solomon, M.M., 2018, Evaluation of chitosan and carboxymethyl cellulose as ecofriendly corrosion inhibitors for steel, *Int. J. Biol. Macromol.*, 117, 1017–1028.

[17] Qiang, A.Y., Zhang, S., Yan, S., Zou, X., and Chen, S., 2017, Three indazole derivatives as corrosion inhibitors of copper in a neutral chloride solution, *Corros. Sci.*, 126, 295–304.

[18] Baari, M.J., Bundjali, B., and Wahyuningrum, D., 2020, Synthesis of oligosuccinimide and evaluation of its corrosion inhibition performance on carbon steel in CO_2-saturated 1% NaCl solution, *J. Math. Fundam. Sci.*, 52 (2), 202–221.

[19] Baari, M.J., Bundjali, B., and Wahyuningrum, D., 2021, Performance of *N,O*-carboxymethyl chitosan as corrosion and scale inhibitors in CO_2-saturated brine solution, *Indones. J. Chem.*, 21 (4), 954–967.

[20] Somers, A.E., Hinton, B.R.W., de Bruin-Dickason, C., Deacon, G.B., Junk, P.C., and Forsyth, M., 2018, New, environmentally friendly, rare earth carboxylate corrosion inhibitors for mild steel, *Corros. Sci.*, 139, 430–437.

[21] Biswas, A., Pal, S., and Udayabhanu, G., 2015, Experimental and theoretical studies of xanthan gum and its graft co-polymer as corrosion inhibitor for mild steel in 15% HCl, *Appl. Surf. Sci.*, 353, 173–183.

[22] Qiang, Y., Zhang, S., Zhao, H., Tan, B., and Wang, L., 2019, Enhanced anticorrosion performance of copper by novel *N*-doped carbon dots, *Corros. Sci.*, 161, 108193.

[23] Cen, H., Zhang, X., Zhao, L., Chen, Z., and Guo, X., 2019, Carbon dots as effective corrosion inhibitor for 5052 aluminium alloy in 0.1 M HCl solution, *Corros. Sci.*, 161, 108197.

[24] Song, Y., Zhu, C., Song, J., Li, H., Du, D., and Lin, Y., 2017, Drug-derived bright and color-tunable *N*-doped carbon dots for cell imaging and sensitive detection of Fe^{3+} in living cells, *ACS Appl. Mater. Interfaces*, 9 (8), 7399–7405.

[25] Jiang, K., Sun, S., Zhang, L., Lu, Y., Wu, A., Cai, C., and Lin, H., 2015, Red, green, and blue luminescence by carbon dots: Full-color emission tuning and multicolor cellular imaging, *Angew. Chem., Int. Ed.*, 54 (18), 5360–5363.

[26] Tao, S., Song, Y., Zhu, S., Shao, J., and Yang, B., 2017, A new type of polymer carbon dots with high quantum yield: From synthesis to investigation on fluorescence mechanism, *Polymer*, 116, 472–478.

[27] Guo, L., Li, L., Liu, M., Wan, Q., Tian, J., Huang, Q., Wen, Y., Liang, S., Zhang, X., and Wei, Y., 2018, Bottom-up preparation of nitrogen doped carbon quantum dots with green emission under microwave-assisted hydrothermal treatment and their biological imaging, *Mater. Sci. Eng., C*, 84, 60–66.

[28] Zhang, H., Huang, H., Ming, H., Li, H., Zhang, L., Liu, Y., and Kang, Z., 2012, Carbon quantum dots/Ag_3PO_4 complex photocatalysts with enhanced photocatalytic activity and stability under visible light, *J. Mater. Chem.*, 22 (21), 10501–10506.

[29] Pan, L., Sun, S., Zhang, A., Jiang, K., Zhang, L., Dong, C., Huang, Q., Wu, A., and Lin, H., 2015, Truly fluorescent excitation-dependent carbon dots and their applications in multicolor cellular imaging and multidimensional sensing, *Adv. Mater.*, 27 (47), 7782–7787.

[30] Roy, P., Chen, P.C., Periasamy, A.P., Chen, Y.N., and Chang, H.T., 2015, Photoluminescent carbon nanodots: Synthesis, physicochemical properties and

analytical applications, *Mater. Today*, 18 (8), 447–458.

[31] Yang, Z., Xu, M., Liu, Y., He, F., Gao, F., Su, Y., Wei, H., and Zhang, Y., 2014, Nitrogen-doped, carbon-rich, highly photoluminescent carbon dots from ammonium citrate, *Nanoscale*, 6 (3), 1890–1895.

[32] Wang, Y., and Hu, A., 2014, Carbon quantum dots: Synthesis, properties and applications, *J. Mater. Chem. C*, 2 (34), 6921–6939.

[33] Xia, C., Zhu, S., Feng, T., Yang, M., and Yang, B., 2019, Evolution and synthesis of carbon dots: From carbon dots to carbonized polymer dots, *Adv. Sci.*, 6 (23), 1901316.

[34] Arukalam, I.O., Madufor, I.C., Ogbobe, O., and Oguzie, E.E., 2014, Inhibition of mild steel corrosion in sulfuric acid medium by hydroxyethyl cellulose, *Chem. Eng. Commun.*, 202 (1), 112–122.

[35] Shen, J., Zhang, T., Cai, Y., Chen, X., Shang, S., and Li, J., 2017, Highly fluorescent *N,S*-co-doped carbon dots: Synthesis and multiple applications, *New J. Chem.*, 41 (19), 11125–11137.

[36] Dang, D.K., Sundaram, C., Ngo, Y.L.T., Chung, J.S., Kim, E.J., and Hur, S.H., 2018, One pot solid-state synthesis of highly fluorescent *N* and *S* co-doped carbon dots and its use as fluorescent probe for Ag^+ detection in aqueous solution, *Sens. Actuators, B*, 255, 3284–3291.

[37] Zhu, C., Fu, Y., Liu, C., Liu, Y., Hu, L., Liu, J., Bello, I., Li, H., Liu, N., Guo, S., Huang, H., Lifshitz, Y., Lee, S.T., and Kang, Z., 2017, Carbon dots as fillers inducing healing/self-healing and anticorrosion properties in polymers, *Adv. Mater.*, 29 (32), 1701399.

[38] Pathak, R.K., and Mishra, P., 2016, Drugs as corrosion inhibitors: A review, *Int. J. Sci. Res.*, 5 (4), 671–677.

[39] Salleh, N.I.H., and Abdullah, A., 2019, Corrosion inhibition of carbon steel using palm oil leaves extract, *Indones. J. Chem.*, 19 (3), 747–752.

[40] Cui, M., Ren, S., Xue, Q., Zhao, H., and Wang, L., 2017, Carbon dots as new eco-friendly and effective corrosion inhibitor, *J. Alloys Compd.*, 726, 680–692.

[41] Xiang, Y., Long, Z., Li, C., Huang, H., and He, X., 2017, Inhibition of N80 steel corrosion in impure supercritical CO_2 and CO_2-saturated aqueous phases by using imino inhibitors, *Int. J. Greenhouse Gas Control*, 63, 141–149.

[42] Wang, W.C., Natelson, R.H., Stikeleather, L.F., and Roberts, W.L., 2012, CFD simulation of transient stage of continuous countercurrent hydrolysis of canola oil, *Comput. Chem. Eng.*, 43, 108–119.

[43] Tamalmani, K., and Husin, H., 2020, Review on corrosion inhibitors for oil and gas corrosion issues, *Appl. Sci.*, 10 (10), 3389.

[44] Ye, Y., Zou, Y., Jiang, Z., Yang, Q., Chen, L., Guo, S., and Chen, H., 2020, An effective corrosion inhibitor of *N* doped carbon dots for Q235 steel in 1 M HCl solution, *J. Alloys Compd.*, 815, 152338.

[45] Liu, Z., Ye, Y.W., and Chen, H., 2020, Corrosion inhibition behavior and mechanism of *N*-doped carbon dots for metal in acid environment, *J. Cleaner Prod.*, 270, 122458.

[46] Zhu, M., He, Z., Guo, L., Zhang, R., Anadebe, V.C., Obot, I.B., and Zheng, X., 2021, Corrosion inhibition of eco-friendly nitrogen-doped carbon dots for carbon steel in acidic media: Performance and mechanism investigation, *J. Mol. Liq.*, 342, 117583.

[47] Cui, M., Ren, S., Zhao, H., Wang, L., and Xue, Q., 2018, Novel nitrogen doped carbon dots for corrosion inhibition of carbon steel in 1 M HCl solution, *Appl. Surf. Sci.*, 443, 145–156.

[48] Saraswat, V., and Yadav, M., 2020, Carbon Dots as green corrosion inhibitor for mild steel in HCl solution, *ChemistrySelect*, 5 (25), 7347–7357.

[49] Ye, Y., Yang, D., Chen, H., Guo, S., Yang, Q., Chen, L., Zhao, H., and Wang, L., 2020, A high-efficiency corrosion inhibitor of *N*-doped citric acid-based carbon dots for mild steel in hydrochloric acid environment, *J. Hazard. Mater.*, 381, 121019.

[50] Yang, D., Ye, Y., Su, Y., Liu, S., Gong, D., and Zhao, H., 2019, Functionalization of citric acid-based carbon dots by imidazole toward novel green corrosion inhibitor for carbon steel, *J. Cleaner Prod.*, 229, 180–192.

[51] Cao, S., Liu, D., Wang, T., Ma, A., Liu, C., Zhuang, X., Ding, H., Mamba, B.B., and Gui, J., 2021, Nitrogen-doped carbon dots as high-effective

inhibitors for carbon steel in acidic medium, *Colloids Surf., A*, 616, 126280.

[52] Cao, C., 1996, On electrochemical techniques for interface inhibitor research, *Corros. Sci.*, 38 (12), 2073–2082.

[53] Anindita, F., Darmawan, N., and Mas'ud, Z.A., 2018, Fluorescence carbon dots from durian as an eco-friendly inhibitor for copper corrosion, *AIP Conf. Proc.*, 2014, 020008.

[54] Ye, Y., Yang, D., and Chen, H., 2019, A green and effective corrosion inhibitor of functionalized carbon dots, *J. Mater. Sci. Technol.*, 35 (10), 2243–2253.

[55] Li, J., Lv, J., Fu, L., Tang, M., and Wu, X., 2020, New ecofriendly nitrogen-doped carbon quantum dots as effective corrosion inhibitor for saturated CO_2 3% NaCl solution, *Russ. J. Appl. Chem.*, 93 (3), 380–392.

[56] Cui, M., Qiang, Y., Wang, W., Zhao, H., and Ren, S., 2021, Microwave synthesis of eco-friendly nitrogen doped carbon dots for the corrosion inhibition of Q235 carbon steel in 0.1 M HCl, *Int. J. Electrochem. Sci.*, 16, 151019.

[57] Cui, M., Yu, Y., and Zheng, Y., 2021, Effective corrosion inhibition of carbon steel in hydrochloric acid by dopamine-produced carbon dots, *Polymers*, 13 (12), 1923.

[58] Luo, J., Cheng, X., Zhong, C., Chen, X., Ye, Y.W., Zhao, H., and Chen, H., 2021, Effect of reaction parameters on the corrosion inhibition behavior of *N*-doped carbon dots for metal in 1 M HCl solution, *J. Mol. Liq.*, 338, 116783.

[59] Xu, Q., Ge, K., Zhang, S., and Tan, B., 2021, Understanding the adsorption and inhibitive properties of nitrogen-doped carbon dots for copper in 0.5 M H_2SO_4 solution, *J. Taiwan Inst. Chem. Eng.*, 125, 23–34.

[60] Zhang, Y., Zhang, S., Tan, B., Guo, L., and Li, H., 2021, Solvothermal synthesis of functionalized carbon dots from amino acid as an eco-friendly corrosion inhibitor for copper in sulfuric acid solution, *J. Colloid Interface Sci.*, 604, 1–14.

[61] Luo, J., Cheng, X., Chen, X., Zhong, C.F., Xie, H., Ye, Y.W., Zhao, H.C., Li, Y., and Chen, H., 2021, The effect of *N* and *S* ratios in *N,S* co-doped carbon dot inhibitor on metal protection in 1 M HCl solution, *J. Taiwan Inst. Chem. Eng.*, 127, 387–398.

[62] Zhu, M., Guo, L., He, Z., Marzouki, R., Zhang, R., and Berdimurodov, E., 2022, Insights into the newly synthesized *N*-doped carbon dots for Q235 steel corrosion retardation in acidizing media: A detailed multidimensional study, *J. Colloid Interface Sci.*, 608, 2039–2049.

[63] Pan, L., Li, G., Wang, Z., Liu, D., Zhu, W., Tong, C., Zhu, R., and Hu, S., 2021, Carbon dots as environment-friendly and efficient corrosion inhibitors for Q235 steel in 1 M HCl, *Langmuir*, 37 (49), 14336–14344.

[64] Saraswat, V., Kumari, R., and Yadav, M., 2022, Novel carbon dots as efficient green corrosion inhibitor for mild steel in HCl solution: Electrochemical, gravimetric and XPS studies, *J. Phys. Chem. Solids*, 160, 110341.

[65] Hosseini, S.M.A., Salari, M., Jamalizadeh, E., Khezripoor, S., and Seifi, M., 2010, Inhibition of mild steel corrosion in sulfuric acid by some newly synthesized organic compounds, *Mater. Chem. Phys.*, 119 (1-2), 100–105.

[66] Kahyarian, A., and Nesic, S., 2019, A new narrative for CO_2 corrosion of mild steel, *J. Electrochem. Soc.*, 166 (11), C3048–C3063.

[67] Li, J.X., Schieberle, P., and Steinhaus, M., 2017, Insights into the key compounds of durian (*Durio zibethinus L.* 'Monthong') pulp odor by odorant quantitation and aroma simulation experiments, *J. Agric. Food Chem.*, 65 (3), 639–647.

[68] Ashassi-Sorkhabi, H., Majidi, M.R., and Seyyedi, K., 2004, Investigation of inhibition effect of some amino acids against steel corrosion in HCl solution, *Appl. Surf. Sci.*, 225 (1-4), 176–185.

[69] Hu, Z., Meng, Y., Ma, X., Zhu, H., Li, J., Li, C., and Cao, D., 2016, Experimental and theoretical studies of benzothiazole derivatives as corrosion inhibitors for carbon steel in 1 M HCl, *Corros. Sci.*, 112, 563–575.

[70] Liu, J., Wang, D., Gao, L., and Zhang, D., 2016, Synergism between cerium nitrate and sodium dodecylbenzenesulfonate on corrosion of AA5052

aluminium alloy in 3 wt.% NaCl solution, *Appl. Surf. Sci.*, 389, 369–377.

[71] Abdallah, M., Sobhi, M., and Altass, H.M., 2016, Corrosion inhibition of aluminum in hydrochloric acid by pyrazinamide derivatives, *J. Mol. Liq.*, 223, 1143–1150.

[72] Li, X., Deng, S., and Xie, X., 2014, Experimental and theoretical study on corrosion inhibition of oxime compounds for aluminium in HCl solution, *Corros. Sci.*, 81, 162–175.

[73] Dariva, C.G., and Galio, A.F., 2014, "Corrosion Inhibitors – Principles, Mechanisms and Applications" in *Developments in Corrosion Protection*, Eds. Aliofkhazraei, M., IntechOpen, Rijeka, Croatia, 365–379.

[74] Yaro, A.S., Khadom, A.A., and Ibraheem, H.F., 2011, Peach juice as an anti-corrosion inhibitor of mild steel, *Anti-Corros. Methods Mater.*, 58 (3), 116–124.

[75] Issaadi, S., Douadi, T., and Chafaa, S., 2014, Adsorption and inhibitive properties of a new heterocyclic furan Schiff base on corrosion of copper in HCl 1M: Experimental and theoretical investigation, *Appl. Surf. Sci.*, 316, 582–589.

[76] Rudnick, L.R., 2009, *Lubricant Additives: Chemistry and Applications*, 2nd Ed., CRC Press, USA.

[77] Tang, Z., 2019, A review of corrosion inhibitors for rust preventative fluids, *Curr. Opin. Solid State Mater. Sci.*, 23 (4), 100759.

[78] Fayomi, O.S.I., Anawe, P.A.L., and Daniyan, A., 2018, "The Impact of Drugs as Corrosion Inhibitors on Aluminum Alloy in Coastal-Acidified Medium, in Corrosion Inhibitors, Principles and Recent Applications" in *Corrosion Inhibitors, Principles and Recent Applications*, Eds. Aliofkhazraei, M., IntechOpen, Rijeka, Croatia, 81–94.

[79] Berdimurodov, E., Kholikov, A., Akbarov, K., Xu, G., Abdullah, A.M., and Hosseini, M., 2020, New anti-corrosion inhibitor (3ar,6ar)-3a,6a-di-p-tolyltetrahydroimidazo[4,5-d]imidazole-2,5(1 h,3h)-dithione for carbon steel in 1 M HCl medium: gravimetric, electrochemical, surface and quantum chemical analyses, *Arabian J. Chem.*, 13 (10), 7504–7523.

[80] Khadiri, A., Saddik, R., Bekkouche, K., Aouniti, A., Hammouti, B., Benchat, N., Bouachrine, M., and Solmaz, R., 2016, Gravimetric, electrochemical and quantum chemical studies of some pyridazine derivatives as corrosion inhibitors for mild steel in 1 M HCl solution, *J. Taiwan Inst. Chem. Eng.*, 58, 552–564.

[81] Anejjar, A., Salghi, R., Zarrouk, A., Benali, O., Zarrok, H., Hammouti, B., and Ebenso, E.E., 2014, Inhibition of carbon steel corrosion in 1 M HCl medium by potassium thiocyanate, *J. Assoc. Arab Univ. Basic Appl. Sci.*, 15, 21–27.

[82] Ferreira, E.S., Giacomelli, C., Giacomelli, F.C., and Spinelli, A., 2004, Evaluation of the inhibitor effect of L-ascorbic acid on the corrosion of mild steel, *Mater. Chem. Phys.*, 83 (1), 129–143.

[83] Behpour, M., Ghoreishi, S.M., Soltani, N., and Salavati-Niasari, M., 2009, The inhibitive effect of some bis-*N,S*-bidentate Schiff bases on corrosion behaviour of 304 stainless steel in hydrochloric acid solution, *Corros. Sci.*, 51 (5), 1073–1082.

[84] Wang, D., Li, Y., Chen, B., and Zhang, L., 2020, Novel surfactants as green corrosion inhibitors for mild steel in 15% HCl: Experimental and theoretical studies, *Chem. Eng. J.*, 402, 126219.

[85] Ismail, A., Irshad, H.M., Zeino, A., and Toor, I.H., 2019, Electrochemical corrosion performance of aromatic functionalized imidazole inhibitor under hydrodynamic conditions on API X65 carbon steel in 1 M HCl solution, *Arabian J. Sci. Eng.*, 44 (6), 5877–5888.

[86] Goni, L.K.M.O., Mazumder, M.A.J., Ali, S.A., Nazal, M.K., and Al-Muallem, H.A., 2019, Biogenic amino acid methionine-based corrosion inhibitors of mild steel in acidic media, *Int. J. Miner. Metall. Mater.*, 26 (4), 467–482.

[87] Wahyuningrum, D., Achmad, S., Syah, Y.M., Buchari, B., and Ariwahjoedi, B., 2008, The Synthesis of imidazoline derivative compounds as corrosion inhibitor towards carbon steel in 1% NaCl solution, *ITB J. Sci.*,40 (1), 33–48.

[88] Li, X., Deng, S., Lin, T., Xie, X., and Du, G., 2019, Cassava starch ternary graft copolymer as a

corrosion inhibitor for steel in HCl solution, *Integr. Med. Res.*, 9 (2), 2196–2207.

[89] Lahrour, S., Benmoussat, A., Bouras, B., Mansri, A., Tannaouga, L., and Marzorati, S., 2019, Glycerin-grafted starch as corrosion inhibitor of C-Mn steel in 1 M HCl solution, *Appl. Sci.*, 9 (21), 4684.

[90] Baari, M.J., and Sabandar, C.W., 2021, A Review on expired drug-based corrosion inhibitors: chemical composition, structural effects, inhibition mechanism, current challenges, and future prospects, *Indones. J. Chem.*, 21 (5), 1316–1336.

[91] Singh, P., Chauhan, D.S., Srivastava, K., Srivastava, V., and Quraishi, M.A., 2017, Expired atorvastatin drug as corrosion inhibitor for mild steel in hydrochloric acid solution, *Int. J. Ind. Chem.*, 8 (4), 363–372.